Oligonucleotides Containing Pyrazolo[3,4-*d*]pyrimidines: The Influence of 7-Substituted 8-Aza-7-deaza-2′-deoxyguanosines on the Duplex Structure and Stability

by **Frank Seela*** and **Georg Becher**

Laboratorium für Organische und Bioorganische Chemie, Institut für Chemie, Universität Osnabrück, Barbarastrasse 7, D-49069 Osnabrück, Germany
(Fax: + 49(541)969-2370, e-mail: Fraseela@rz.uni-osnabrueck.de)

Oligonucleotides containing 7-substituted 8-aza-7-deazaguanines (= 6-amino-1,5-dihydro-4*H*-pyrazolo[3,4-*d*]pyrimidin-4-ones) were prepared by automated solid-phase synthesis. A series of 7-alkynylated 8-aza-7-deaza-2′-deoxyguanosines (see **4a**–**d**) were synthesized with the 7-iodonucleoside **3c** as starting material and by the Pd^0/Cu^I-catalyzed cross-coupling reaction with various alkynes. Phosphoramidites were prepared from the 7-substituted 8-aza-7-deaza-2′-deoxyguanosine derivatives carrying halogeno, cyano, and hexynyl substituents. From the melting profiles of oligonucleotide duplexes, the T_m values as well as the thermodynamic data were determined. A significant duplex stabilization by the 7-substituents was observed for the DNA · DNA duplexes, but not in the case of DNA · RNA hybrids.

1. Introduction. – Pyrazolo[3,4-*d*]pyrimidines (= 8-aza-7-deazapurines; see **A** in *Fig. 1*) combine structural elements of purines (see **C**) [1] and pyrrolo[2,3-*d*]pyrimidines (7-deazapurines; see **B**) [2][3]. All three heterocyclic systems are constructed from a pyrimidine moiety which takes part in the *Watson-Crick* base pairing of nucleic acids. Unlike the purines, the pyrrolo[2,3-*d*]pyrimidines and the pyrazolo[3,4-*d*]pyrimidines possess a five-membered ring with a 7-position (purine numbering is used throughout the discussion section) which can be functionalized with substituents differing in size and electronegativity.

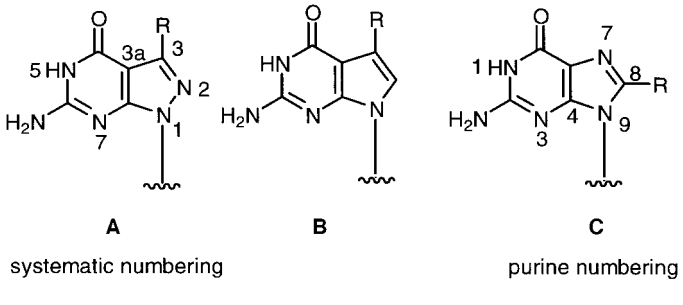

Fig. 1. *Structures of purine analogues*

When 8-aza-7-deazapurines replace purines in nucleic acids, isomorphous *Watson-Crick* base pairs are formed, with a bidentate structure in the case of the 8-aza-7-deazaadenine · thymine pair, or a tridentate motif in the case of a 8-aza-7-

deazaguanine · cytosine pair [4][5]. The 7-substituents of 8-aza-7-deazapurines, like the 8-substituents of purines, are directed towards the major groove of the B-DNA, similarly to those of pyrrolo[2,3-*d*]pyrimidines. Model building shows that rather bulky substituents are well accommodated in the major groove of the DNA. Furthermore, it was demonstrated in the case of 7-substituted 8-aza-7-deazaadenines [6] that these substituents stabilize the DNA duplex structure [7][8]. This is at variance with 8-substituted purines; their substituents interfere sterically with the sugar-phosphate backbone, thereby destabilizing DNA duplexes [9].

The present investigation reports on the influence of 7-substituents of 8-aza-7-deazaguanines such as alkynyl groups, halogen atoms, or a carbamoyl residue on the DNA duplex structure and stability. The synthesis of the phosphoramidites **1a**–**d** and **2** is described, and self-complementary and non-self-complementary oligonucleotides are prepared. Their duplex stability is investigated and compared with that of RNA · DNA hybrids. Part of the work has been reported earlier in form of an abstract [10] and in a short communication [11].

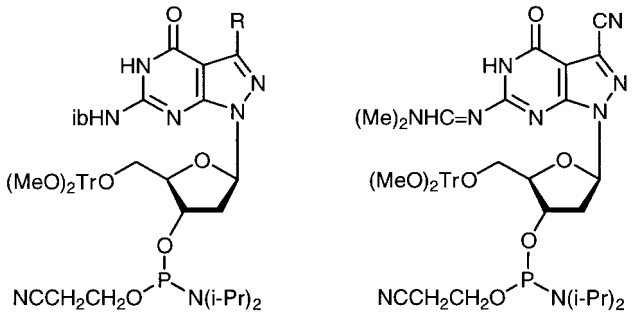

1a R = H
b R = Br
c R = I
d R = hxy

ib = Me_2CHCO

2

2. Results and Discussion. – 2.1. *Monomers.* – The synthesis of 8-aza-7-deaza-2′-deoxyguanosine [12] as well as of its 7-bromo, 7-iodo, and 7-cyano derivatives [13][14] has been described elsewhere. The 7-alkynylated derivatives **4a**–**d** were prepared from 8-aza-7-deaza-2′-deoxy-7-iodoguanosine (**3c**) and terminal alkynes by the Pd^0-catalyzed cross coupling [15] (*Scheme 1*). The reaction was performed in DMF with tetrakis(triphenylphosphine)palladium(0), copper(I) iodide, and Et_3N under Ar. After chromatographic workup, the desired 7-alkynyl-8-aza-7-deaza-2′-deoxyguanosines **4a**–**d** were isolated and characterized. The increasing lipophilic character of the 7-iodo derivative (**3c**) and the 7-alkynyl derivatives **4a**–**c** – compared with the parent nucleoside **3a** – is demonstrated in *Fig. 2*, and the chromatographic mobility of the cyano nucleoside **3d** as well as of the carbamoyl derivative **3e** is shown in *Fig. 3*.

From X-ray studies of the halogenated nucleosides **3b**,**c** it is known that these nucleosides possess a very particular conformation around the *N*-glycosylic bond (high-*anti*) different from that of 2′-deoxyguanosine (*syn*) [16]. This is the result of a steric

Scheme 1

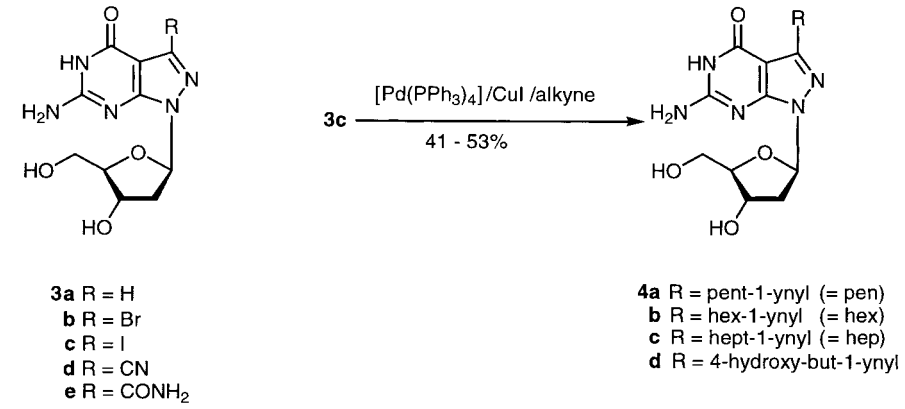

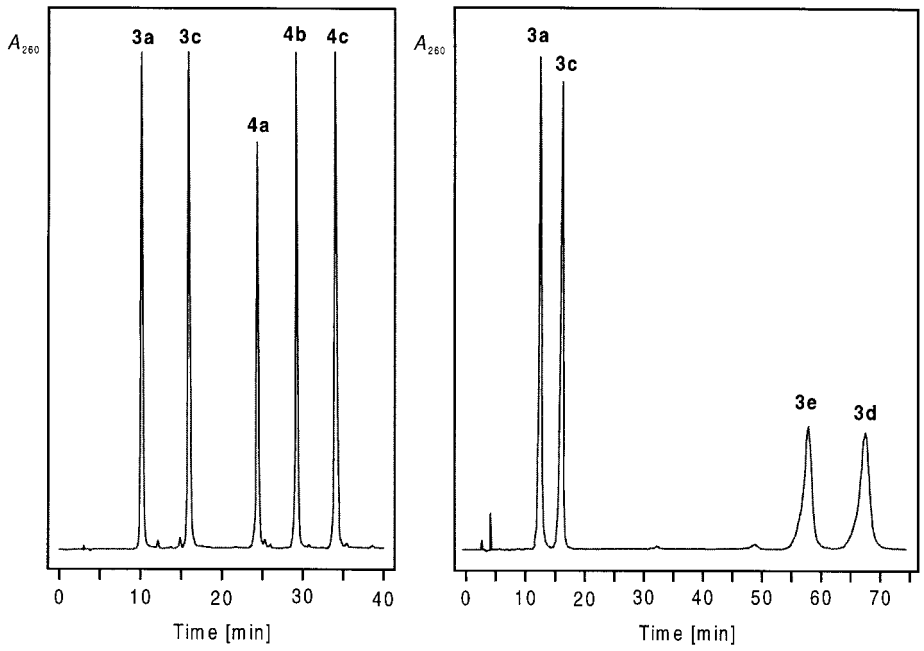

Fig. 2 (left). *HPLC Profile of the nucleosides* **3a**, **3c**, *and* **4a**–**c** *on a* RP-18 (200 × 10 mm) *column.* The following solvent systems were used: MeCN (*A*) and 0.1M (Et_3NH)OAc (pH 7.0)/MeCN 95 : 5 (*B*). Gradient: 20 min 5–20% *A* in *B*, 40 min 20–40% *A* in *B*.

Fig. 3 (right). *HPLC Profile of the nucleosides* **3a**, **3c**, *and* **3d** *on a* RP-18 (200 × 10 mm) *column.* Solvent system, see *Fig. 2*. Gradient: 0–75 min, 100% *B*.

and stereoelectronic influence of the nucleobase on the sugar moiety, which can alter the secondary structure of single-stranded and double-stranded oligonucleotides [17]. Compared to 2′-deoxyguanosine, 8-aza-7-deaza-2′-deoxyguanosine (**3a**) shows a slightly destabilized *N*-glycosylic bond when it is hydrolyzed in acidic medium [12].

As acidic conditions are used for the 4,4′-dimethoxytrityl ($(MeO)_2Tr$) group removal during oligonucleotide synthesis, the glycosylic-bond stability of the nucleosides **3a–d** and **4b** was investigated. The hydrolysis of the 7-substituted derivatives was performed in 0.5N HCl at room temperature. The reaction was followed UV-spectrophotometrically at 254 nm as well as by HPLC analysis. From *Table 1* it is apparent that the halogenated and alkynylated derivatives **3b**, **c** and **4a–c** show an about ten-fold higher glycosylic-bond stability than the parent 8-aza-7-deaza-2′-deoxyguanosine (**3a**). The glycosylic bonds of the 7-cyano and the 7-carbamoyl derivatives **3d**,**e** are stable under these conditions. When these compounds were hydrolyzed at 40° and at a higher HCl concentration, hydrolysis was observed (*Table 1*). This phenomenon can be explained by the electron-withdrawing character of the 7-substituents. It corresponds to the σ_{para} *Hammett* values (alkynyl = 0.03 < iodo = 0.18 < bromo = 0.23 < carbamoyl = 0.36 < cyano = 0.66) [18a]. According to this, the *pK* values of protonation are reduced and the nucleobase looses its ability to form a protonated species. As protonation of the base is necessary for the *N*-glycosylic-bond hydrolysis, the increased stability of the 7-substituted derivatives of *Table 1* becomes understandable [18b]. The stabilizing effect of electron-withdrawing substituents observed in pyrazolo[3,4-*d*]pyrimidine nucleosides is opposite to that found for 8-substituted purine nucleosides. In acidic medium, 8-bromo-2′-deoxyguanosine depurinates much faster than 2′-deoxyguanosine [19].

Table 1. *Half-life Values* (τ) *of 2′-Deoxyguanosine Derivatives in 0.5*N *HCl at 25°*

	τ [min][a])		τ [min]
dG [4]	11	$CONH_2{}^7c{}^7z{}^8G_d$ (**3e**)	stable[b])
$c^7z^8G_d$ (**3a**) [4]	4	$CN^7c^7z^8G_d$ (**3d**)	stable[b])
$Br^7c^7z^8G_d$ (**3b**) [13]	44	$CONH_2{}^7c{}^7z{}^8G_d$ (**3e**)	58[c])
$I^7c^7z^8G_d$ (**3c**) [13]	47	$CN^7c^7z^8G_d$ (**3d**)	29[d])
$pen^7c^7z^8G_d$ (**4a**)	34		
$hxy^7c^7z^8G_d$ (**4b**)	36		
$hep^7c^7z^8G_d$ (**4c**)	36		

[a]) Measured in 0.5N HCl at 25°. [b]) Within 3 h. [c]) Measured in 0.5N HCl at 40°. [d]) Measured in 2N HCl at 40°.

For the preparation of oligonucleotides containing the modified bases, an appropriate protecting group has to be selected. Two series of protecting groups were studied. In analogy to 8-aza-7-deaza-2′-deoxyguanosine (**3a**), compounds **3b–c** and **4b** were protected at the amino group with the isobutyryl residue (ib) employing the protocol of transient protection (*Scheme 2*) [20]: the products **5a–d** were isolated in 63–67% yield. The amidines **7a–d** were obtained from the reaction of the nucleosides with dimethylformamide dimethyl acetal [21]. The kinetics of deprotection was determined UV-spectrophotometrically in 25% ammonia (40°) at 310 nm for the amidines and at 300 nm for the acyl derivatives. *Table 2* summarizes the half-life values of the base-catalyzed deprotection. According to this, the *N*-isobutyryl (ib) protecting group of the nucleosides **5a–d** is less stable than that of the analogous purine [22]. The half-lives of deprotection of the amidines **7a–d** are shorter than those of the acyl derivatives but do not differ significantly among themselves.

Next, the protected intermediates **5a–d** and **7d** were converted to the 4,4′-dimethoxytrityl derivatives **6a–d** and **8** (69–74% yield), respectively, by standard

Scheme 2

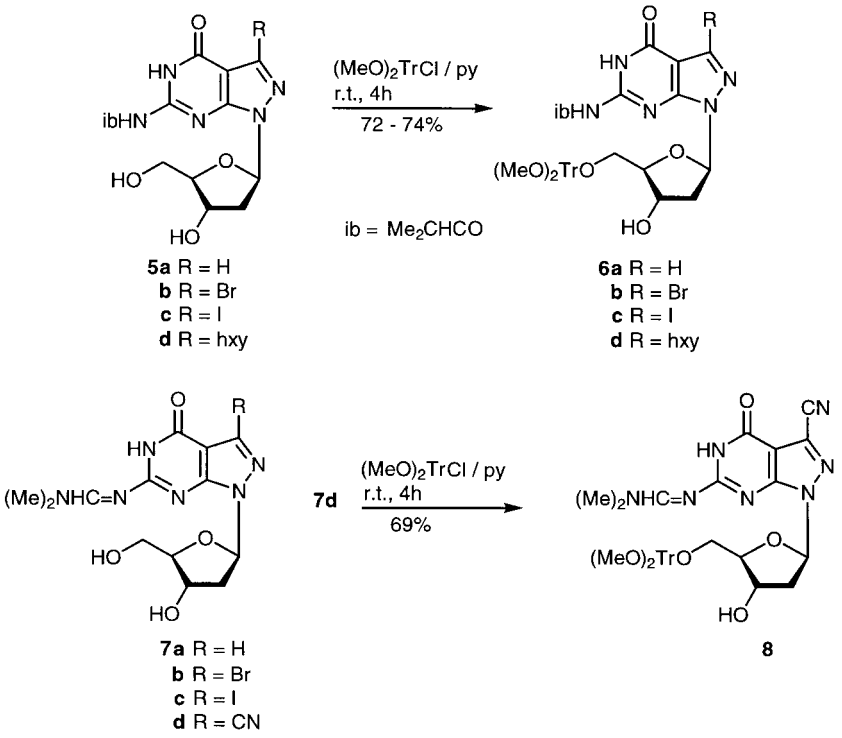

Table 2. *Half-life Values* (τ) *of Amino-Protected 2′-Deoxyguanosine Derivatives in 25% aq. Ammonia at 40°*

	τ [min][a])		τ [min][b])
ib^2G_d [4]	112	$m_2fa^2G_d$ [4]	19
$ib^2c^7z^8G_d$ (**5a**)	31	$m_2fa^2c^7z^8G_d$ (**7a**)	16
$ib^2Br^7c^7z^8G_d$ (**5b**)	38	$m_2fa^2Br^7c^7z^8G_d$ (**7b**)	16
$ib^2I^7c^7z^8G_d$ (**5c**)	41	$m_2fa^2I^7c^7z^8G_d$ (**7c**)	19
$ib^2hex^7c^7z^8G_d$ (**5d**)	27	$m_2fa^2CN^7c^7z^8G_d$ (**7d**)	18

[a]) Measured UV spectrophotometrically at 300 nm. [b]) Measured at 310 nm.

reaction conditions [23]. Phosphitylation [24] of **6a**–**d** and **8**, performed in THF in the presence of chloro(2-cyanoethyl)(diisopropylamino)phosphine (= 2-cyanoethyl diisopropylphosphoroamidochloridite) and $(i\text{-}Pr)_2EtN$ [25], furnished the phosphoramidites **1a**–**d** and **2**, respectively, which were purified by FC and isolated as colorless foams (78–79% yield).

All compounds were characterized by ^1H-, ^{13}C-, and ^{31}P-NMR spectra and by elemental analysis (*Table 3* and *Exper. Part*). *Table 3* summarizes the ^{13}C-NMR data.

The introduction of a substituent in the 7-position (derivatives **3b**–**e** and **4a**–**c**) leads to a significant upfield shift of the C(7) signal. It is most pronounced in the case of the iodo compound **3c** (33 ppm); the 7-bromo and the 7-cyano derivatives **3b**,**d** show similar chemical shifts. The upfield shift of the alkynyl derivatives **4a**–**c** is small (4.5 ppm). The formamidines **7a**–**d** show two well-separated signals for the Me resonance in the ^{13}C-NMR

Table 3. *^{13}C-NMR Chemical Shifts of Pyrazolo[3,4-*d*]pyrimidine 2′-Deoxyribonucleosides*[a])

	C(3)[b]) C(7)[c])	C(3a) C(5)	C(4)[d]) C(6)	C(6)[d]) C(2)	C(7a)[d]) C(4)	C=O	C=N	*C*≡C	C≡*C*	C≡N	C(1′)	C(2′)	C(3′)	C(4′)	C(5′)
3a [4]	134.9	99.7	157.4	154.6	155.2						83.1	37.9	71.0	87.3	62.4
b	122.0	98.4	158.1	156.3	156.5						83.1	37.6	70.8	87.4	62.4
c	101.9	93.7	157.5	155.1	156.8						83.2	37.7	70.9	87.5	62.4
d	119.2	101.4	156.3	155.9	155.9					113.9	84.0	37.9	70.8	88.0	62.2
4a	130.4	100.0	156.9	155.1	155.4			93.3	73.2		83.1	37.7	70.9	87.5	62.4
b	130.4	100.0	156.9	155.1	155.4			93.4	72.9		83.1	37.6	70.9	87.5	62.4
c	130.4	100.0	156.9	155.1	155.4			93.5	73.0		83.1	37.7	70.9	87.5	62.4
d	130.4	100.1	157.6	155.6	155.6			91.5	73.8		83.1	37.7	71.0	87.6	62.5
5a [4]	135.7	102.9	155.9	150.2	152.9	180.6					83.6	37.9	71.0	87.8	62.5
b	122.3	101.6	154.8	150.7	153.7	180.6					83.7	37.7	70.7	87.7	62.2
c	105.1	94.1	155.3	150.2	153.2	180.6					83.6	37.8	70.7	87.7	62.2
d	130.7	103.0	155.0	158.0	152.7	180.5		94.6	72.3		83.6	39.0	70.8	87.7	62.2
6a [4]	135.7	103.0	155.9	150.1	152.8	180.7					83.7	38.2	70.8	85.6	64.4
b	122.2	101.8	154.8	150.6	153.5	180.6					83.9	38.0	70.5	85.7	64.1
c	105.4	94.2	155.5	150.3	153.3	180.7					84.1	38.2	70.7	85.8	64.4
d	130.6	103.1	155.0	150.3	152.6	180.6		94.3	72.4		83.8	39.1	70.3	85.1	63.9
7a [4]	135.3	102.3	159.2	158.6	154.7		158.6				83.3	38.1	71.3	87.7	62.6
b	121.9	100.7	159.6	157.5	155.3		158.6				83.2	37.8	70.9	87.5	62.3
c	104.1	93.6	159.1	150.4	154.9		158.6				83.3	37.9	70.9	87.5	62.3
d	119.9	104.6	161.0	157.9	155.9		159.9			113.9	85.0	38.9	71.6	88.8	63.0
8	118.9	103.7	160.2	149.5	154.8		159.0			113.0	83.9	38.3	63.9	85.7	63.9

[a]) Measured in (D_6)DMSO at 298 K. [b]) Systematic numbering. [c]) Purine numbering. [d]) Tentative.

as well as in the ^{1}H-NMR spectra (34.8 and 40.8 ppm, and 3.10 and 3.30 ppm, resp.). The assignment of C(2), C(4), and C(6) is tentative. To verify the assignment of the C(1′) and C(4′) signals of the sugar moiety, gated-decoupled ^{13}C-NMR spectra where measured, and C(1′) was assigned according to its larger coupling constant.

Regarding the ^{1}H-NMR spectra, the carbamoyl nucleoside **3e** (identical with structure **D**) shows peculiarities. As it will be shown in the case of the oligonucleotides **35**, **36** (see *2.2.1*), **3e** was obtained by conversion of the 7-cyano substituent to the 7-carbamoyl group upon treatment with ammonia (**3d** → **3e**). A similar conversion has been observed for 7-cyano-7-deaza-2′-deoxyadenosine [26]. In the ^{1}H-NMR spectrum ((D_6)DMSO) of **3e** the amide protons are split into two *s* (7.74, 9.51 ppm). This results from the formation of the H-bonded structure **D**. The signal at lower field is assigned to the amide proton, which is part of the seven-membered ring. The corresponding pyrrolo[2,3-*d*]pyrimidine nucleoside shows also two signals (7.08 and 9.54 ppm, resp.) for the amide protons [14], which indicates the formation of structure **E**.

2.2. *Oligonucleotides.* 2.2.1. *Synthesis and Characterization*. Automated solid-phase synthesis of the oligonucleotides **9** – **39** (see below, *Tables 5* – *8*) was performed with the phosphoramidites **1a** – **d** and **2** as well as the standard phosphoramidites. The synthesis protocol has been described [27], and the coupling yields were always >95%. The oligonucleotides were detritylated and purified on oligonucleotide-purification cartridges [28]. The oligonucleotide with a 3′-terminal pyrazolo[3,4-*d*]pyrimidine moiety, *i.e.* **13**, was synthesized on a universal support with a 3′-terminal ribose moiety [29]. The removal of this residue was achieved upon prolonged treatment with ammonia or in the presence of LiCl. The homogeneity of the compounds was established by ion-exchange

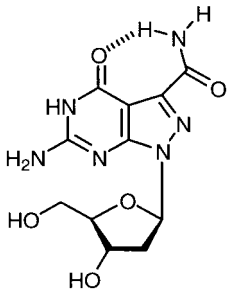

Structure **D**

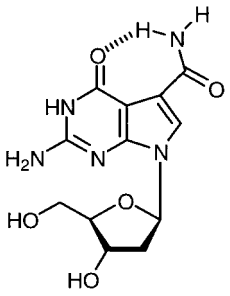

Structure **E**

chromatography on a *NucleoPac-PA-100* column (4×50 mm; *Dionex*, P/N 043018, USA). The composition of the oligonucleotides was determined by tandem hydrolysis with snake-venom phosphodiesterase and alkaline phosphatase as described [8]. From the modified oligonucleotides **11**, **12**, **15**–**18**, **24**–**26**, and **29**–**38**, MALDI-TOF mass spectra were taken (*Table 4*).

Table 4. *Molecular Weights of Oligonucleotides* **11**, **12**, **15**–**18**, **24**–**26**, *and* **29**–**38**, *from MALDI-TOF Mass Spectra*

Oligomer	M^+ (calc.)	M^+ (found)
5′-d[(**3b**-C)$_3$]-3′(**11**)	2030.0	2033.0
5′-d[(**3c**-C)$_3$]-3′(**12**)	2170.9	2171.0
5′-d[(**3a**-C)$_4$]-3′(**15**)	2411.6	2412.3
5′-d[(**3b**-C)$_4$]-3′(**16**)	2727.2	2727.6
5′-d[(**3c**-C)$_4$]-3′(**17**)	2917.5	2915.3
5′-d[(**4b**-C)$_4$]-3′(**18**)	2732.2	2733.2
5′-d(**3a**TA**3a**AATTCTAC)-3′ (**24**)	3644.4	3647.7
5′-d(**3b**TA**3b**AATTCTAC)-3′ (**25**)	3800.2	3803.0
5′-d(**3c**TA**3c**AATTC TAC)-3′ (**26**)	3896.2	3901.2
5′-d(TA**3a3a**TCAATACT)-3′ (**29**)	3644.4	3645.1
3′-d(ATCCA**3a**TTAT**3a**A)-5′ (**30**)	3644.4	3644.6
5′-d(TA**3b3b**TCAATACT)-3′ (**31**)	3800.2	3805.6
3′-d(ATCCA**3b**TTAT**3b**A)-5′ (**32**)	3800.2	3802.4
5′-d(TA**3c3c**TCAATACT)-3′ (**33**)	3896.2	3897.5
3′-d(ATCCA**3c**TTAT**3c**A)-5′ (**34**)	3896.2	3893.1
5′-d(TA**4b4b**TCAATACT)-3′ (**37**)	3802.1	3806.4
3′-d(ATCCA**4b**TTAT**4b**A)-5′ (**38**)	3802.1	3805.6
5′-d(TA**3e3e**TCAATACT)-3′ (**35**)	3830.2	3831.0
3′-d(ATCCA**3e**TTAT**3e**A)-5′ (**36**)	3830.2	3827.0

The oligoribonucleotide **39** was a generous gift of Dr. *L. Beigelman* [30]. When the phosphoramidite **2** was employed in solid-phase synthesis and the oligonucleotides were deprotected with ammonia, the 7-cyano group was converted to a carbamoyl group. The enzymatic hydrolysis resulted – apart from the peaks of the standard nucleosides – in a new peak of the modified nucleoside **3e** and not of the nitrile **3d** (*Fig. 4*). Furthermore, the MALDI-TOF mass spectrum of the oligonucleotides **35**–**36** gave the masses that correspond to the presence of the carbamoyl function and not of the cyano group.

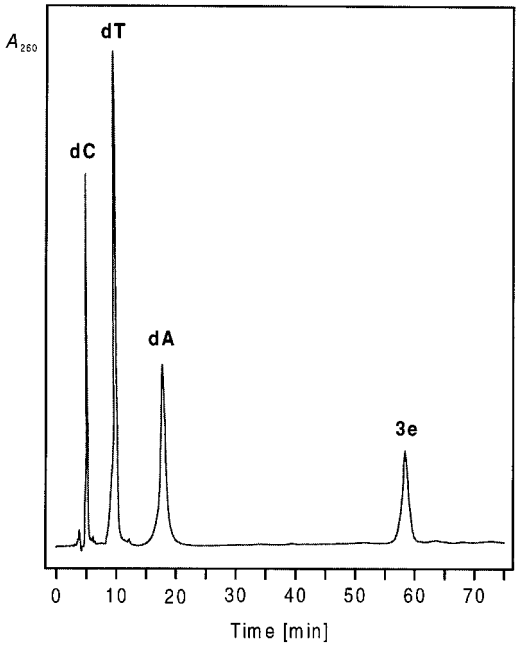

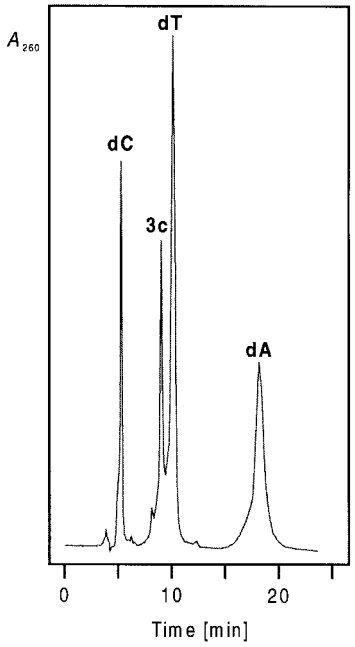

Fig. 4 (left). *HPLC Profile of the reaction products obtained after enzymatic hydrolysis of the oligonucleotide* **35** *by snake-venom phosphodiesterase and alkaline phosphatase in* 1M Tris·*HCl buffer* (pH 8.1) *at 37°*. Column: *RP-18* (200 × 10 mm); gradient: 0–75 min 100% *B* (see *Fig. 2*).

Fig. 5 (right). *HPLC Profile of the reaction products obtained after enzymatic hydrolysis of the oligonucleotide* **33** *by snake-venom phosphodiesterase and alkaline phosphatase in* 1M Tris·*HCl buffer* (pH 8.1) *at 37°*. Column: *RP-18* (200 × 10 mm); gradient: 0–20 min 100% *B* (see *Fig. 2*).

2.2.2. *Properties.* Regarding duplex stability, different types of oligonucleotide duplexes were studied: *i*) the self-complementary duplexes derived from alternating dG-dC, *ii*) the palindromic structures derived from 5′-d(GGAATTCC)-3′ (see **19**·**19**) or 5′-d(GTAGAATTCTAC) (see **23**·**23**) and *iii*) the non-self-complementary hybrids derived from the duplex 5′-d(TAGGTCAATACT)-3′·3′-d(ATCCAGTTATGA)-5′ (**27**·**28**). Also DNA·RNA hybrids were investigated in the case of the non-self-complementary duplexes.

DNA·DNA Duplexes. From *Table 5* it is apparent that the incorporation of the 8-aza-7-deazapurine nucleosides **3a**–**c** into the self-complementary oligomers **9**–**13** leads to a significant increase of the T_m values [31–34]. Already the replacement of the guanine residues by the non-substituted 8-aza-7-deazaguanine **3a** (oligomer **10**) results in a T_m increase of 15° compared to the parent oligonucleotide **9** containing guanines. When the 7-halogenated derivatives **3b**,**c** are introduced (see hexamers **11**–**13**), an additional increase of the melting temperature ($\Delta T_m = 7-10°$) is found. The nucleoside **3a** increases the stability of the duplex structure **9**·**9** by 2.5° per base residue, whereas the contribution of the 7-halogenated nucleosides **3b**,**c** is higher (*ca.* 4° per base replacement).

The same tendency as observed for the self-complementary hexamer oligonucleotides is found for the alternating octamers **14**–**18**. The duplex **15**·**15** shows a notably

Table 5. T_m *Values, Thermodynamic Data, and Thermal Hypochromicities for the Self-Complementary Oligonucleotides* **9**–**18** *with Alternating Bases*[a])

	Duplex	T_m [°C]	ΔH^0 [kcal/mol]	ΔS^0 [cal/mol K]	ΔG^0_{298} [kcal/mol]	H_{260} [%]	H_{272} [%]
5′-d[(G-C)$_3$ J-3′ (**9**)	**9**·**9**	47	−55	−150	−8.4		19
5′-d[(**3a**-C)$_3$J-3′ (**10**)	**10**·**10**	62	−64	−175	−12.0		13
5′-d[(**3b**-C)$_3$J-3′ (**11**)	**11**·**11**	72	−59	−149	−13.1	4	10
5′-d[(**3c**-C)$_3$ J-3′ (**12**)	**12**·**12**	72	−62	−162	−12.9	10	9
5′-d[(C-**3c**)$_3$ J-3′ (**13**)	**13**·**13**	71	−59	−149	−12.4		7
5′-d[(G-C)$_4$ J-3′ (**14**)	**14**·**14**	63	−68	−180	−12.1	5	22
5′-d[(**3a**-C)$_4$J-3′ (**15**)	**15**·**15**	73	−74	−193	−14.5	2	15
5′-d[(**3b**-C)$_4$J-3′ (**16**)	**16**·**16**	88	[b])	[b])	[b])	[b])	[b])
5′-d[(**3c**-C)$_4$ J-3′ (**17**)	**17**·**17**	84	[b])	[b])	[b])	[b])	[b])
5′-d[(**4b**-C)$_4$J-3′ (**18**)	**18**·**18**	83	−78	−196	−16.8	11	

[a]) Measured in 0.1M NaCl, 10 mM $MgCl_2$, and 10 mM Na-cacodylate at pH 7, between 20–100°, the oligomer concentration was 20 μM for the hexamers **9**–**13** and 15 μM for the octamers **14**–**18**. [b]) Not detectable.

higher T_m value ($\Delta T_m = 10°$) than that of the parent purine oligomer **14**·**14** (*Table 5*). The 7-bromo- and 7-iodo substituents of the 8-aza-7-deazaguanine lead to further stabilization (see **16** and **17**). It is surprising to see that this stabilizing effect is accompanied by a decrease in the thermal hypochromicity (272 nm). As the hypochromicity is normally used as a measure for base stacking, one would expect the opposite. However, even with the help of thermodynamic data, the situation seems to be complex and might depend on the particular electronic properties of the pyrazolo[3,4-*d*]pyrimidine nucleosides.

Similar results as observed for the self-complementary oligonucleotide duplexes of *Table 5* were found for the palindromic oligodeoxyribonucleotides **19**–**26** (see *Table 6*). The incorporation of **3a** leads to a stabilization of the duplex **19**·**19** and **23**·**23** (+1° per residue). An additional increase of the T_m value is observed when the halogenated nucleosides **3b**,**c** are introduced (2.2–2.5° per incorporated residue). To exclude hairpin formation of the self-complementary oligonucleotides, the concentration dependence of the T_m values was measured. The thermodynamic data observed by this method are in fairly good agreement with the data obtained by curve-shape analysis (*Table 6*).

Table 6. T_m *Values, Thermodynamic Data, and Thermal Hypochromicities for the Self-Complementary Palindromic Oligonucleotides* **19**–**26**[a])

	Duplex	T_m [°C]	ΔH^0 [kcal/mol]	ΔS^0 [cal/mol K]	ΔG^0_{298} [kcal/mol]	H_{260} [%]
5′-d(GGAATTCC)-3′ (**19**)	**19**·**19**	31	−63	−184	−5.8	19
5′-d(**3a3a**AATTCC)-3′ (**20**)	**20**·**20**	38	−55	−155	−7.1	21
5′-d(**3b3b**AATTCC)-3′ (**21**)	**21**·**21**	43	−69	−197	−8.1	19
5′-d(**3c3c**AATTCC)-3′ (**22**)	**22**·**22**	43	−47	−126	−7.9	15
5′-d(GTAGAATTCTAC)-3′ (**23**)	**23**·**23**	43	−84	−225	−8.6	23
5′-d(**3a**TA**3a**AATTCTAC)-3′ (**24**)	**24**·**24**	46	−82	−232	−9.6	19
5′-d(**3b**TA**3b**AATTC TAC)-3′ (**25**)	**25**·**25**	52	−76	−211	−10.7	23
5′-d(**3c**TA**3c**AATTC TAC)-3′ (**26**)	**26**·**26**	52	−73 (−84)[b])	−201 (236)[b])	−10.4 (−10.9)[b])	22

[a]) Conditions, see *Table 5*, with 5+5 μM single-strand concentration. [b]) Determined by concentration-dependent measurements; plot: $1/T_m$ *vs.* ln *c* and calculated with the *Meltwin* program [37].

Next, the non-self-complementary duplexes derived from 5′-d(TAGGTCAA-TACT)-3′ (**27**) and 5′-d(AGTATTGACCTA)-3′ (**28**) with a random base composition (see **29**–**38**) were investigated (see *Table 7*). The duplex **27**·**28** was used as a standard in our laboratory, and its T_m value was determined to be 46°. An enhanced stability of DNA duplexes is found in the case of the 7-substituted 8-aza-7-deazaguanines. Already the non-substituted **3a** increases the T_m value significantly (see **29**·**30**). The T_m increase by the 7-substituted derivatives is 2–2.5° per base residue, whereas the non-substituted 8-aza-7-deazaguanine stabilizes the duplex by 1° per residue.

Table 7. T_m *Values, Thermodynamic Data, and Thermal Hypochromicities of the Hetero Duplexes Formed from* **27**–**38**[a])

	Duplex	T_m [°C]	ΔH^0 [kcal/mol]	ΔS^0 [cal/mol K]	ΔG^0_{298} [kcal/mol]	H_{260} [%]
5′-d(TAGGTCAATACT)-3′ (**27**) 3′-d(ATCCAGTTATGA)-5′ (**28**)	**27**·**28**	46	−82	−230	−10.4	17
5′-d(TA**3a3a**TCAATACT)-3′ (**29**) 3′-d(ATCCA**3a**TTAT**3a**A)-5′(**30**)	**29**·**30**	50	−93	−263	−11.8	18
5′-d(TA**3b3b**TCAATACT)-3′ (**31**) 3′-d(ATCCA**3b**TTAT**3b**A)-5′ (**32**)	**31**·**32**	55	−78	−219	−14.3	19
5′-d(TA**3c3c**TCAATACT)-3′ (**33**) 3′-d(ATCCA**3c**TTAT**3c**A)-5′ (**34**)	**33**·**34**	54	−79	−217	−14.2	19
5′-d(TA**3e3e**TCAATACT)-3′ (**35**) 3′-d(ATCCA**3e**TTAT**3e**A)-5′ (**36**)	**35**·**36**	56	−87	−240	−13.2	21
5′-d(TA**4b4b**TCAATACT)-3′ (**37**) 3′-d(ATCCA**4b**TTAT**4b**A)-5′ (**38**)	**37**·**38**	53	−119	−338	−14.0	21

[a]) Measured in 0.1M NaCl, 10 mM $MgCl_2$, and 10 mM Na-cacodylate at pH 7; 5 + 5 μM single strand concentration.

The CD spectra of the duplexes containing 8-aza-7-deazaadenines (see *Figs. 6* and *7*) indicate a B-like DNA structure (see, *e.g.*, **31**·**32**, **33**·**34**, and **35**·**36** as well as **37**·**38** in *Fig. 8*). They show a positive *Cotton* effect around either 270 or 290 nm and a negative lobe at 250 nm. The CD spectrum of the duplex **17**·**17** containing 8-aza-7-deaza-7-iodoguanine shows significant differences to the others. Similar differences were reported for the 7-substituted 8-aza-7-deaza-7-iodoadenine [6].

DNA·*RNA Duplexes.* Duplexes which contain one DNA and one RNA strand are important molecules in the cellular machinery. They are formed during the reverse transcription of viral RNA from DNA. They occur when RNA polymerase transcribes DNA to messenger RNA and are formed during DNA replication (*Okazaki* fragments). Finally, the antisense therapeutics are based on hybrids formed between synthetic DNA with messenger RNA. Generally, an RNA·RNA duplex is more stable than a DNA·DNA duplex. The stability of DNA·RNA hybrids is less than those of RNA·RNA or DNA·DNA. However, the stability depends also on other factors, *e.g.*, on the content of the adenine·thymine (uracil) base pairs. Special effects are observed when a DNA or an RNA duplex contains stretches of adenines [35].

To study the influence of 7-substituents of 8-aza-7-deazaguanines on the stability of DNA·RNA hybrids, the oligodeoxyribonucleotides **27**, **29**, **31**, and **33** were hybridized with the oligoribonucleotide **39**; for comparison, the hybridization was also performed with the oligodeoxyribonucleotide **28** (see *Table 8*). *Table 8* shows that the various modifications exert very little influence on the duplex stability of DNA·RNA hybrids, except that the 8-aza-7-deazaguanine slightly destabilizes the duplex compared to the

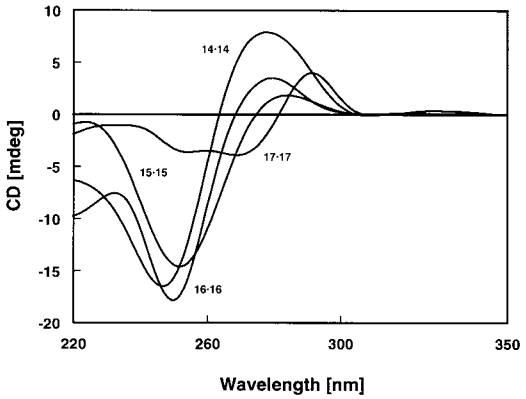

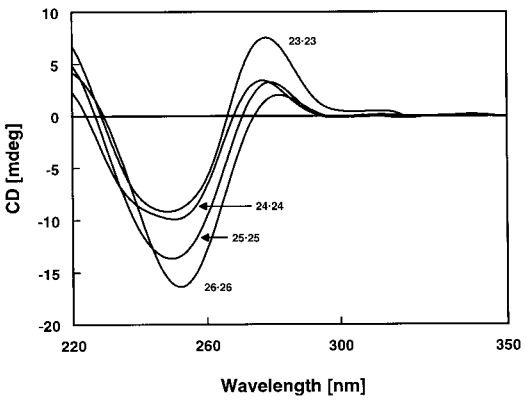

Fig. 6 (left). *CD Spectra of the alternating duplexes* **14**·**14**, **15**·**15**, **16**·**16**, *and* **17**·**17**. Measured at 20° in 0.1M NaCl, 10 mM $MgCl_2$, and 10 mM Na-cacodylate at pH 7 with 5 + 5 μM oligomer concentration.

Fig. 7 (right). *CD Spectra of the palindromic duplexes* **23**·**23**, **24**·**24**, **25**·**25**, *and* **26**·**26**. Measured at 20° in 0.1M NaCl, 10 mM $MgCl_2$, and 10 mM Na-cacodylate at pH 7 with 5 + 5 μM oligomer concentration at 260 nm.

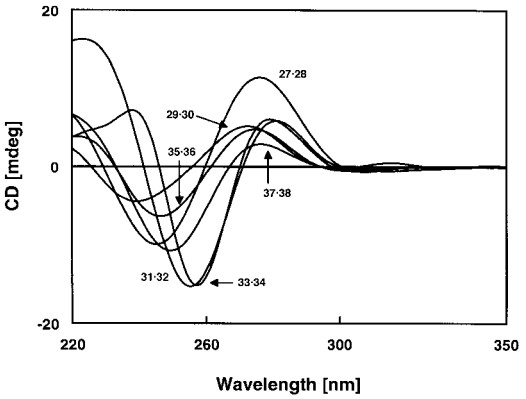

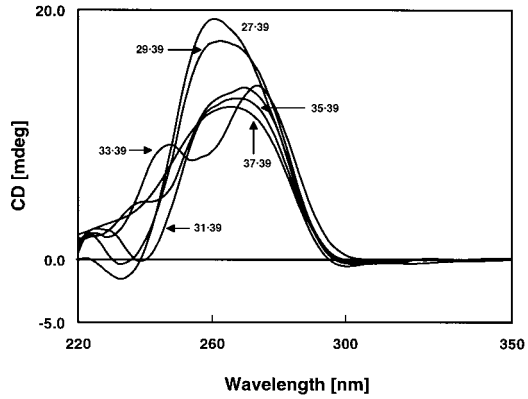

Fig. 8 (left). *CD Spectra of the hetero duplexes* **27**·**28**, **29**·**30**, **31**·**32**, **33**·**34**, **35**·**36**, *and* **37**·**38**. Measured at 20° in 0.1M NaCl, 10 mM $MgCl_2$, and 10 mM Na-cacodylate at pH 7 with 5 + 5 μM oligomer concentration

Fig. 9 (right). *CD Spectra of the RNA*·*DNA duplexes* **27**·**39**, **29**·**39**, **31**·**39**, **33**·**39**, **35**·**39**, *and* **37**·**39**. Measured at 20° in 0.1M NaCl, 10 mM $MgCl_2$, and 10 mM Na-cacodylate at pH 7 with 5 + 5 μM oligomer concentration at 260 nm without consideration of the thermal hypochromicity.

parent guanine. By way of contrast, the DNA·DNA duplexes containing the same number of modified bases at exactly the same positions of the oligonucleotide chain show a significant T_m increase which correlates with the stabilities of duplexes containing four modified residues. The hypochromicities of the chimeric hybrids are slightly decreased over those of the DNA·DNA duplexes.

From the CD spectra it can be seen that the DNA duplexes are in a B-like form (*Figs. 8* and *9*), while the DNA·RNA hybrids adopt the A-form [36] (*Fig. 9*). Normally, the A-RNA form has a very deep major and a shallow minor groove. In DNA·RNA hybrids, the minor groove is in an intermediate stage. It is difficult to interpret the stability differences observed in the DNA·DNA and the DNA·RNA

Table 8. T_m *Values, Thermodynamic Data, and Thermal Hypochromicities of RNA · DNA and DNA · DNA Hybrids*[a])

	Duplex	T_m [°C]	ΔH^0 [kcal/mol]	ΔS^0 [cal/mol K]	ΔG^0_{298} [kcal/mol]	H_{260} [%]
5′-d(TAGGTCAATACT)-3′ (**27**) 3′-(AUCCAGUUAUGA)-5′ (**39**)	**27 · 39**	45	– 92	– 264	– 10.2	20
5′-d(TA**3a3a**TCAATACT)-3′ (**29**) 3′-dAUCCAGUUAUGA)-5′ (**39**)	**29 · 39**	44	– 87	– 248e	– 9.9	21
5′-d(TA**3b3b**TCAATACT)-3′ (**31**) 3′-(AUCCAGUUAUGA)-5′ (**39**)	**31 · 39**	47	– 90	– 256	– 10.7	21
5′-d(TA**3c3c**TCAATACT)-3′ (**33**) 3′-(AUCCAGUUAUGA)-5′ (**39**)	**33 · 39**	46	– 84	– 238	– 10.3	21
5′-d(TA**3e3e**TCAATACT)-3′ (**38**) 3′-(AUCCAGUUAUGA)-5′ (**39**)	**38 · 39**	47	– 82	– 230	– 10.5	20
5′-d(TA**4b4b**TCAATACT)-3′ (**36**) 3′-(AUCCAGUUAUGA)-5′ (**39**)	**36 · 39**	46	– 87	– 249	– 10.2	20
5′-d(TAGGTCAATACT)-3′ (**27**) 3′-d(ATCCAGTTATGA)-5′ (**28**)	**27 · 28**	46	– 82	– 230	– 10.4	17
5′-d(TA**3a3a**TCAATACT)-3′ (**29**) 3′-d(ATCCAGTTATGA)-5′ (**28**)	**29 · 28**	48	– 91	– 258	– 11.3	17
5′-d(TA**3b3b**TCAATACT)-3′ (**31**) 3′-d(ATCCAGTTATGA)-5′ (**28**)	**31 · 28**	52	– 105	– 301	– 12.4	18
5′-d(TA**3c3c**TCAATACT)-3′ (**33**) 3′-d(ATCCAGTTATGA)-5′ (**28**)	**33 · 28**	52	– 104	– 298	– 12.4	17
5′-d(TA**3e3e**TCAATACT)-3′ (**35**) 3′-d(ATCCAGTTATGA)-5′ (**28**)	**35 · 28**	51	– 95	– 268	– 11.9	18
5′-d(TA**4b4b**TCAATACT)-3′ (**37**) 3′-d(ATCCAGTTATGA)-5′ (**28**)	**37 · 28**	50	– 111	– 317	– 12.3	16

[a]) Conditions, see *Table 7*.

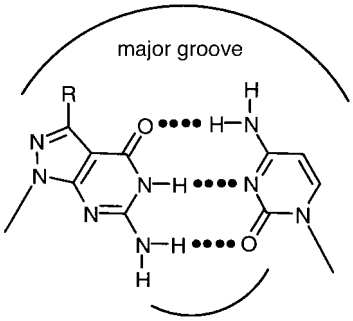

Base-pair motif **F**

R = H, Br, I, hxy, $CONH_2$

series. However, neither the hydrophobicity of the 7-substituents, which might displace H_2O molecules, nor the electron-withdrawing properties, which affect stacking, play a significant role in the stability of the DNA · RNA hybrids shown in *Table 8*.

In conclusion, the 7-substituents of 8-aza-7-deazaguanine are well accommodated in DNA · DNA duplexes, in DNA · RNA hybrids, and possibly also in duplex RNA. The

DNA · DNA duplexes are significantly stabilized by the 7-substituents and form tridentade base pairs of the *Watson-Crick* type (base-pair motif **F**). Little influence is observed in the case of DNA · RNA hybrids. Nevertheless, even the bulky 7-iodo substituent does not decrease the stability of such a hybrid. Consequently, the introduction of large reporter groups will be possible without affecting the duplex structure when these groups are attached to the 7-position of 8-aza-7-deazaguanines in DNA as well as in RNA.

We thank Dr. *H. Rosemeyer* and *H. Debelak* for helpful discussions. We also appreciate the supply of MALDI-TOF data by Dr. *T. Wenzel* (*Bruker Saxonia*, Leipzig) and Mrs. *J. Gross* from the group of Prof. *Hillenkamp*, Universität Münster. Financial support by the *Deutsche Forschungsgemeinschaft* is gratefully acknowledged.

Experimental Part

General. See [6]. Flash chromatography (FC): 0.4 bar on silica gel *60 H* (*Merck*, Darmstadt, Germany). Thin-layer chromatography (TLC): aluminium sheets coated with silica gel *60* F_{254} (0.2 mm; *Merck*, Germany). Solvent systems for FC and TLC: CH_2Cl_2/MeOH 95 :5 (*A*), CH_2Cl_2/MeOH 9 :1 (*B*), CH_2Cl_2/acetone 9 :1 (*C*); CH_2Cl_2/acetone 8 :2 (*D*), CH_2Cl_2/AcOEt/Et_3N 75 :14 :1 (*E*). M.p.: *Büchi-SMP-20* apparatus (*Büchi*, Switzerland); not corrected. NMR Spectra: *AC-250* and *AMX-500* spectrometers (*Bruker*, Germany); δ values in ppm downfield from internal $SiMe_4$ (^1H, ^{13}C). Microanalyses were performed by *Mikroanalytisches Labor Beller*, Göttingen, Germany.

Oligonucleotides. Oligonucleotide synthesis was performed on a DNA synthesizer, model *392*, *Applied Biosystems*, Weiterstadt, Germany. Melting curves were measured with a *Cary-1/3* UV/VIS spectrophotometer (*Varian*, Australia) equipped with a *Cary* thermoelectrical controller. The actual temperature was measured in the reference cell with a Pt-100 resistor. CD Spectra: *Jasco-600* (*Jasco*, Japan) spectropolarimeter; thermostatically (*Lauda-RCS-6* bath) controlled 1-cm cuvettes. UV Spectra: *150-20* spectrometer (*Hitachi*, Japan).

The enzymatic hydrolysis of the oligonucleotides was performed as described in [6] with the following extinction coefficients: ε_{260}: dT 8800, dC 7300, dA 15400, dG 11700. Snake-venom phosphodiesterase (EC 3.1.15.1, *Crotallus durissus*) and alkaline phosphatase (EC 3.1.3.1, *E. coli*) were generous gifts from *Roche Diagnostics GmbH*.

*Pd-Catalyzed Cross Coupling of 6-Amino-1-(2-deoxy-β-*D-erythro-*pentofuranosyl)-1,5-dihydro-3-iodo-4*H-*pyrazolo[3,4-*d*]pyrimidin-4-one* (**3c**) *with Terminal Alkynes: General Procedure.* A suspension of **3c** (200 mg, 0.51 mmol) and CuI (19.5 mg, 0.1 mmol) in anh. DMF (2 ml) was treated with alkyne (10 equiv.), anh. Et_3N (104 mg, 0.1 mmol), and $[Pd(PPh_3)_4]$ (59 mg, 0.052 mmol). The mixture was stirred under Ar (→ clear yellow soln.) until the starting material was consumed (TLC monitoring). The mixture was diluted with MeOH/CH_2Cl_2 1 :1 (5 ml), and *Dowex 1* × *8* (100 – 200 mesh; 500 mg hydrogen carbonate form) was added. After stirring for 15 min, the evolution of gas ceased. Stirring was continued for another 30 min, the mixture filtered, and the resin washed with MeOH/CH_2Cl_2 1 :1 (50 ml). The combined filtrate was evaporated and the residue chromatographed (silica gel column (10 × 8 cm), CH_2Cl_2 with 10, 15, and then 20% of MeOH). The main zone afforded the desired nucleoside.

*6-Amino-1-(2-deoxy-β-*D-erytho-*pentofuranosyl)-1,5-dihydro-3-(pent-1-ynyl)-4*H-*pyrazolo[3,4-*d*]pyrimidin-4-one* (**4a**): Colorless solid (88 mg, 52%). TLC (*B*): R_f 0.2. UV (MeOH): 243 (34500). ^{1}H-NMR ((D$_6$)DMSO): 1.02 (*t*, *J* = 7.3, *Me*CH_2); 1.58 (2*m*, MeCH_2); 2.51 (*m*, 1 H–C(2′)); 2.43 (*t*, *J* = 7.0, ≡C–CH_2); 2.66 (*m*, 1 H–C(2′)); 3.38 (*m*, 2 H–C(5′)); 3.77 (*m*, H–C(3′)); 4.36 (*m*, H–C(4′)); 4.96 (*t*, *J* = 6.5, OH–C(5′)); 5.19 (*d*, *J* = 3.2, OH–C(3′)); 6.28 (‘*t*’, *J* = 6.4, H–C(1′)); 6.70 (*s*, NH_2); 10.64 (*s*, NH). Anal. calc. for $C_{15}H_{19}N_5O_4$ (333.3): C 54.05, H 5.75, N 21.01; found: C 53.97, H 5.74, N 20.71.

*6-Amino-1-(2-deoxy-β-*D-erytho-*pentofuranosyl)-3-(hex-1-ynyl)-1,5-dihydro-4*H-*pyrazolo[3,4-*d*]pyrimidin-4-one* (**4b**): Colorless solid (87 mg, 49%). TLC (*B*): R_f 0.2. UV (MeOH): 243 (36800). ^{1}H-NMR ((D$_6$)DMSO): 0.90 (*t*, *J* = 7.3, *Me*CH_2); 1.45 – 1.56 (2*m*, CH_2CH_2); 2.14 (*m*, 1 H–C(2′)); 2.44 (*t*, *J* = 8.4, ≡C–CH_2); 2.66 (*m*, 1 H–C(2′)); 3.37 (*m*, 2 H–C(5′)); 3.77 (*m*, H–C(4′)); 4.43 (*m*, H–C(3′)); 4.69 (*t*, *J* = 5.0, OH–C(5′)); 5.19 (*d*, *J* = 3.2, OH–C(3′)); 6.28 (‘*t*’, *J* = 6.4, H–C(1′)); 6.70 (*s*, NH_2); 10.63 (*s*, NH). Anal. calc. for $C_{16}H_{21}N_5O_4$ (347.4): C 55.32, H 6.09, N 20.16; found: C 55.24, H 6.01, N 19.79.

*6-Amino-1-(2-deoxy-β-*D-erytho-*pentofuranosyl)-3-(hept-1-ynyl)-1,5-dihydro-4*H-*pyrazolo[3,4-*d*]pyrimidin-4-one* (**4c**): Colorless solid (98 mg, 53%). TLC (*B*): R_f 0.2. UV (MeOH): 243 (35100). ^{1}H-NMR((D$_6$)DMSO):

0.90 (t, J = 7.3, *Me*CH_2); 1.32 (m, Me*CH_2*); 1.42 (m, CH_2CH_2); 1.56 (m, CH_2CH_2); 2.14 (m, 1 H–C(2′)); 2.44 (t, J = 8.4, ≡C–CH_2); 2.66 (m, 1 H–C(2′)); 3.37 (m, 2 H–C(5′)); 3.77 (m, H–C(3′)); 4.34 (m, H–C(4′)); 4.69 (t, J = 5.0, OH–C(5′)); 5.19 (d, J = 3.2, OH–C(3′)); 6.28 (‘t’, J = 6.4, H–C(1′)); 6.70 (s, NH_2); 10.64 (s, NH). Anal. calc. for $C_{17}H_{23}N_5O_4$ (361.40): C 56.50, H 6.42, N 19.38; found: C 56.38, H 6.47, N 19.26.

*6-Amino-1-(2-deoxy-β-*D-erythro-*pentofuranosyl)-1,5-dihydro-3-(4-hydroxybut-1-ynyl)-4*H*-pyrazolo[3,4-*d*]-pyrimidin-4-one* (**4d**). Colorless solid (70 mg, 41%). TLC (*B*): R_f 0.2. UV (MeOH): 242 834800). ^{1}H-NMR ((D$_6$)DMSO): 215 (m, 1 H–C(2′)); 2.56 (t, J = 7.1, ≡C–CH_2); 2.66 (m, 1 H–C(2′)); 3.45 (m, 2 H–C(5′)); 3.75 (m, H–C(4′)); 4.34 (m, H–C(3′)); 4.71 (t, J = 5.6, OH–C(5′)); 4.89 (t, J = 5.5, CH_2CH_2O*H*); 5.20 (d, J = 3.2, OH–C(3′)); 6.26 (‘t’, J = 6.3, H–C(1′)); 6.60 (s, NH_2); 10.64 (s, NH). Anal. calc. for $C_{14}H_{17}N_5O_5$ (335.32): C 50.15, H 5.11, N 20.89; found: C 50.03, H 5.28, N 20.60.

*3-Bromo-1-(2-deoxy-β-*D-erythro-*pentofuranosyl)-1,5-dihydro-6-[(2-methylpropanoyl)amino]-4*H*-pyrazolo[3,4-*d*]pyrimidin-4-one* (**5b**). Compound **3b** (1.0 g, 2.9 mmol) was dried by co-evaporation with pyridine. The residue was dissolved in DMF (10 ml) and 1,1,1,3,3,3-hexamethyldisilazane (HMDS; 5 ml) was added. Stirring was continued for 3 h, and pyridine (10 ml) and 2-methylpropanoic anhydride (10 ml) were added. The soln. was stirred for additional 12 h, then MeOH (20 ml) was added, and stirring was continued for 3 h. The volume of the soln. was reduced to near dryness, and the crude material was precipitated by the addition of Et_2O/hexane 1:1 (100 ml). Recrystallization from H_2O/MeOH 2:1 gave **5b** (785 mg, 65%). Colorless crystals. M.p. 215°. TLC (*B*): R_f 0.4. UV (MeOH): 225 (13000), 274 (11500). ^{1}H-NMR ((D$_6$)DMSO): 1.11 (d, J = 6.7, *Me*$_2$CH); 2.22 (m, 1 H–C(2′)); 2.70 (m, 1 H–C(2′)); 3.36, 3.46 (m, CH_2(5′)); 3.78 (m, H–C(4′)); 4.38 (m, H–C(3′)); 4.70 (t, J = 5.7, OH–C(5′)); 5.23 (d, J = 4.3, OH–C(3′)); 6.34 (‘t’, J = 6.5, H–C(1)); 11.77 (s, NH); 11.93 (s, NH). Anal. calc. for $C_{14}H_{18}BrN_5O_5$ (416.2): C 40.40, H 4.36, N 16.83; found: C 40.60, H 4.52, N 16.77.

*1-(2-Deoxy-β-*D-erythro-*pentofuranosyl)-1,5-dihydro-3-iodo-6-[(2-methylpropanoyl)amino]-4*H*-pyrazolo[3,4-*d*]-pyrimidin-4-one* (**5c**). As described for **5b**, with **3c** (1.0 g, 2.5 mmol), DMF (10 ml), HMDS (5 ml), pyridine (10 ml), and 2-methylpropanoic anhydride (10 ml): **5c** (775 mg, 67%). Colorless needles. M.p. 213°. TLC (*B*): R_f 0.4. UV (MeOH): 273 (11300). ^{1}H-NMR ((D$_6$)DMSO): 1.11 (d, J = 6.7, *Me*$_2$CH); 2.21 (m, 1 H–C(2′)); 2.73 (m, 1 H–C(2′)); 3.32, 3.46 (m, 2 H–C(5′)); 3.77 (m, H–C(3′)); 4.38 (m, H–C(4′)); 4.70 (t, J = 5.7, OH–C(5′)); 5.25 (d, J = 4.3, OH–C(3′)); 6.31 (‘t’, J = 6.5, H–C(1′)); 12.38 (s, 2 NH). Anal. calc. for $C_{14}H_{18}IN_5O_5$ (463.2): C 36.30, H 3.92, N 15.12; found: C 36.46, H 3.85, N 15.05.

*1-(2-Deoxy-β-*D-erythro-*pentofuranosyl)-3-(hex-1-ynyl)-1,5-dihydro-6-[(2-methylpropanoyl)amino]-4*H*-pyrazolo[3,4-*d*]pyrimidin-4-one* (**5d**). As described for **5b**, with **4b** (300 mg, 0.87 mmol) in DMF (5 ml), HMDS (2.5 ml; 2 h), pyridine (5 ml), and 2-methylpropanoic anhydride (5 ml): **5d** (230 mg, 63%). Colorless needles. M.p. 215°. TLC (*B*): R_f 0.4. UV (MeOH): 250 (20100), 267 (12300). ^{1}H-NMR ((D$_6$)DMSO): 0.92 (t, J = 7.1, *Me*CH_2); 1.13 (d, J = 6.7, *Me*$_2$CH); 1.44–1.57 (2m, CH_2CH_2); 2.22 (m, 1 H–C(2′)); 2.76 (m, 1 H–C(2′)); 3.45 (m, 2 H–C(5′)); 3.80 (m, H–C(3′)); 4.04 (m, H–C(4′)); 4.69 (t, J = 5.0, OH–C(5′)); 5.24 (d, J = 3.2, OH–C(3′)); 6.37 (‘t’, J = 5.9, H–C(1′)); 11.74 (s, NH). Anal. calc. for $C_{20}H_{27}N_5O_5$ (417.46): C 57.54, H 6.52, N 16.78; found: C 57.42, H 6.36, N 16.53.

*3-Bromo-1-(2-deoxy-β-*D-erythro-*pentofuranosyl)-6-{[(dimethylamino)methylidene]amino}-1,5-dihydro-4*H*-pyrazolo[3,4-*d*]pyrimidin-4-one* (**7b**). To a soln. of **3b** (500 mg, 1.45 mmol) in anh. DMF (5 ml), *N*,*N*-dimethylformamide dimethyl acetal (3 ml) was added under stirring, and stirring was continued at 40° for 2 h. The solvent was evaporated, and the oily residue was evaporated with toluene and acetone (twice 2 × 20 ml) to yield a colorless foam. Crystallization from H_2O afforded **7b** (255 mg, 44%). Colorless needles. M.p. 247°. TLC (*B*): R_f 0.35. UV (MeOH): 246 (28000), 300 (33000). ^{1}H-NMR ((D$_6$)DMSO): 2.18 (m, 1 H–C(2′)); 2.67 (m, 1 H–C(2′)); 3.07 (s, MeN); 3.32 (s, MeN); 3.39, 3.51 (m, 2 H–C(5′)); 3.79 (m, H–C(4′)); 4.38 (m, H–C(3′)); 4.70 (t, J = 5.7, OH–C(5′)); 5.25 (d, J = 4.3, OH–C(3′)); 6.43 (‘t’, J = 6.4, H–C(1′)); 8.70 (s, CH); 11.38 (s, NH). Anal. calc. for $C_{13}H_{17}BrN_6O_4$ (401.22): C 38.92, H 4.27, N 20.95; found: C 39.14, H 4.38, N 20.76.

*1-(2-Deoxy-β-*D-erythro-*pentofuranosyl)-6-{[(dimethylamino)methylidene]amino}-1,5-dihydro-3-iodo-4*H*-pyrazolo[3,4-*d*]pyrimidin-4-one* (**7c**). As described for **7b**, with **3c** (500 mg, 1.27 mmol), DMF (5 ml), and *N*,*N*-dimethylformamide dimethyl acetal (3 ml): **7b** (252 mg, 41%). Colorless needles. M.p. 241°. TLC (*B*): R_f 0.35. UV (MeOH): 248 (28000), 301 (32500). ^{1}H-NMR ((D$_6$)DMSO): 2.19 (m, 1 H–C(2′)); 2.70 (m, 1 H–C(2′)); 3.07 (s, MeN); 3.32 (s, MeN); 3.39, 3.51 (m, 2 H–C(5′)); 3.80 (m, H–C(4′)); 4.40 (m, H–C(3′)); 4.69 (t, J = 5.7, OH–C(5′)); 5.24 (d, J = 4.3, HO–C(3′)); 6.41 (‘t’, J = 6.2, H–C(1′)); 8.68 (s, CH); 11.30 (s, NH). Anal. calc. for $C_{13}H_{17}IN_6O_4$ (448.2): C 34.84, H 3.82, N 18.75; found: C 34.73, H 3.82, N 18.34.

*3-Cyano-1-(2-deoxy-β-*D-erythro-*pentofuranosyl)-6-{[(dimethylamino)methylidene]amino}-1,5-dihydro-4*H*-pyrazolo[3,4-*d*]pyrimidin-4-one* (**7d**). As described for **7b**, with **3d** (500 mg, 1.71 mmol), anh. MeOH (5 ml), and *N*,*N*-dimethylformamide dimethyl acetal (8 ml): **7d** (160 mg, 27%). Colorless needles. M.p. 254°. TLC (*B*):

R_f 0.3. UV (MeOH): 252 (26900), 301 (29000). ^{1}H-NMR ((D$_6$)DMSO): 2.27 (*m*, 1 H–C(2′)); 2.74 (*m*, 1 H–C(2′)); 3.09 (*s*, MeN); 3.28 (*s*, MeN); 3.35, 3.51 (*m*, 2 H–C(5′)); 3.80 (*m*, H–C(4′)); 4.41 (*m*, H–C(3′)); 4.71 (*t*, *J* = 5.6, OH–C(5′)); 5.31 (*d*, *J* = 4.3, OH–C(3′)); 6.52 ('*t*', *J* = 6.3, H–C(1′)); 8.73 (*s*, CH); 11.76 (*s*, NH). Anal. calc. for $C_{14}H_{17}N_7O_4$ (347.34): C 48.41, H 4.93, N 28.23; found: C 48.14, H 5.10, N 28.10.

*3-Bromo-1-[2-deoxy-5-*O*-(4,4′-dimethoxytrityl)-β-*D*-*erythro*-pentofuranosyl]-1,5-dihydro-6-[(2-methylpropanoyl)amino]-4*H*-pyrazolo[3,4-*d*]pyrimidin-4-one* (**6b**). Compound **5b** (500 mg, 1.2 mmol) was dried by co-evaporation with anh. pyridine. The residue was dissolved in anh. pyridine (10 ml) and stirred with 4,4′-dimethoxytrityl chloride (540 mg, 1.6 mmol) in the presence of (i-Pr)$_2$EtN (315 ml, 1.8 mmol) for 1.5 h at r.t. The soln. was poured into 5% aq. $NaHCO_3$ soln. (100 ml), the mixture extracted with CH_2Cl_2 (2 × 100 ml), and the combined org. extract dried ($NaSO_4$) and evaporated. FC (*C* followed by *D*) furnished **6b** (645 mg, 75%). Colorless foam. TLC (*A*): R_f 0.25. UV (MeOH): 275 (15500). ^{1}H-NMR ((D$_6$)DMSO): 1.03 (*d*, *J* = 6.7, *Me*$_2$CH); 2.25 (*m*, 1 H–C(2′)); 2.75 (*m*, 1 H–C(2′)); 3.05 (*m*, 2 H–C(5′)); 3.70 (*s*, 2 MeO); 3.95 (*m*, H–C(4′)); 4.44 (*m*, H–C(3′)); 5.30 (*d*, *J* = 4.5, OH–C(3′)); 6.37 ('*t*', *J* = 6.5, H–C(1′)); 6.77–7.16 (2*m*, 13 arom. H); 11.86 (*s*, NH); 11.97 (*s*, NH). Anal. calc. for $C_{35}H_{36}BrN_5O_7$ (718.6): C 58.50, H 5.05, N 9.75; found: C 58.65, H 5.10, N 9.73.

*1-[2-Deoxy-5-*O*-(4,4′-dimethoxytrityl)-β-*D*-*erythro*-pentofuranosyl]-1,5-dihydro-3-iodo-6-[(2-methylpropanoyl)amino]-4*H*-pyrazolo[3,4-*d*]pyrimidin-4-one* (**6c**). As described for **6b**, with **5c** (400 mg, 0.86 mmol), 4,4′-dimethoxytrityl chloride (380 mg, 1.12 mmol), pyridine (3 ml) and (i-Pr)$_2$EtN (225 ml, 1.3 mmol): **6c** (475 mg, 72%). Colorless foam. TLC (*A*): R_f 0.25. UV (MeOH): 276 (16000). ^{1}H-NMR ((D$_6$)DMSO): 1.12 (*d*, *J* = 6.7, *Me*$_2$CH); 2.25 (*m*, 1 H–C(2′)); 2.77 (*m*, 1 H–C(2′)); 3.03 (*m*, 2 H–C(5′)); 3.70 (*s*, 2 MeO); 3.92 (*m*, H–C(3′)); 4.44 (*m*, H–C(4′)); 5.29 (*d*, *J* = 4.2, OH–C(3′)); 6.37 ('*t*', *J* = 5.5, H–C(1′)); 6.76–7.33 (2*m*, 13 arom. H); 11.83 (*s*, NH); 11.92 (*s*, NH). Anal. calc. for $C_{35}H_{36}IN_5O_7$ (765.6): C 54.91, H 4.74, N 9.15; found: C 55.07, H 4.92, N 9.18.

*1-[2-Deoxy-5-*O*-(4,4′-dimethoxytrityl)-β-*D*-*erythro*-pentofuranosyl]-3-(hex-1-ynyl)-1,5-dihydro-6-[(2-methylpropanoyl)amino]-4*H*-pyrazolo[3,4-*d*]pyrimidin-4-one* (**6d**). As described for **6b** with **5d** (570 mg, 1.4 mmol), 4,4′-dimethoxytrityl chloride (570 mg, 1.12 mmol), and pyridine (3 ml): **6d** (730 mg, 79%). Colorless foam. TLC (*A*): R_f 0.3. UV (MeOH): 273 (16500). ^{1}H-NMR ((D$_6$)DMSO): 0.90 (*t*, *J* = 7.3, *Me*CH$_2$); 1.13 (*d*, *J* = 6.7, *Me*$_2$CH); 1.42–1.56 (2*m*, CH$_2$CH$_2$); 2.27 (*m*, 1 H–C(2′)); 2.77 (*m*, 1 H–C(2′)); 3.03 (*m*, 2 H–C(5′)); 3.72 (*s*, 2 MeO); 3.92 (*m*, H–C(4′)); 4.49 (*m*, H–C(3′)); 5.29 (*d*, *J* = 4.2, OH–C(3′)); 6.40 ('*t*', *J* = 5.9, H–C(1′)); 6.78–7.33 (2*m*, 13 arom. H); 11.83 (*s*, NH); 11.92 (*s*, NH). Anal. calc. for $C_{41}H_{45}N_5O_7$ (719.84): C 68.41, H 6.30, N 9.73; found: C 68.56, H 6.45, N 9.80.

*3-Cyano-1-[2-deoxy-5-*O*-(4,4′-dimethoxytrityl)-β-*D*-*erythro*-pentofuranosyl]-1,5-dihydro-6-[(2-methylpropanoyl)amino]-4*H*-pyrazolo[3,4-*d*]pyrimidin-4-one* (**8**). As described for **6b**, with **7d** (140 mg, 0.4 mmol), 4,4′-dimethoxytrityl chloride (178 mg, 0.52 mmol), and pyridine (1.5 ml): **8** (150 mg, 58%). Colorless foam. TLC (*D*): R_f 0.3. UV (MeOH): 275 (15500). ^{1}H-NMR ((D$_6$)DMSO): 2.33 (*m*, 1 H–C(2′)); 2.70 (*m*, 1 H–C(2′)); 2.98 (*s*, MeN, *m*, 2 H–C(5′)); 3.22 (*s*, MeN); 3.73 (*s*, MeO); 3.93 (*m*, H–C(4′)); 4.53 (*m*, H–C(3′)); 5.34 (*d*, *J* = 4.3, OH–C(3′)); 6.76 ('*t*', *J* = 6.3, H–C(1′)); 6.80–7.30 (2*m*, 13 arom. H); 8.76 (*s*, CH); 11.76 (*s*, NH). Anal. calc. for $C_{35}H_{35}N_7O_6$ (649.72): C 64.70, H 5.43, N 15.09; found: C 64.87, H 5.62, N 15.20.

*3-Bromo-1-[2-deoxy-5-*O*-(4,4′-dimethoxytrityl)-β-*D*-*erythro*-pentofuranosyl]-1,5-dihydro-6-[(2-methylpropanoyl)amino]-4*H*-pyrazolo[3,4-*d*]pyrimidin-4-one 3′-(2-Cyanoethyl Diisopropylphosphoramidite)* (**1b**). A soln. of **6b** (300 mg, 0.42 mmol) in dry THF was stirred with (i-Pr)$_2$EtN (140 µl, 0.84 mmol) at r.t. Then, 2-cyanoethyl diisopropylphosphoramidochloridite (125 µl, 0.55 mmol) was added within 2 min. The salt was filtered off, and the soln. washed with sat. aq. $NaHCO_3$ soln., dried ($NaSO_4$), and evaporated. FC (column 10 × 2 cm, *E*) afforded **1b** (312 mg, 81%). Colorless foam. TLC (*E*): R_f 0.9. ^{31}P-NMR ($CDCl_3$): 148.4, 148.5.

*1-[2-Deoxy-5-*O*-(4,4′-dimethoxytrityl)-β-*D*-*erythro*-pentofuranosyl]-1,5-dihydro-3-iodo-6-[(2-methylpropanoyl)amino]-4*H*-pyrazolo[3,4-*d*]pyrimidin-4-one 3′-(2-Cyanoethyl Diisopropylphosphoramidite)* (**1c**). As described for **1b**, with **6c** (300 mg, 0.39 mmol), THF (2 ml), (i-Pr)$_2$EtN (140 µl, 0.84 mmol), and 2-cyanoethyl diisopropylphosphoramidochloridite (125 µl, 0.55 mmol). FC (column 10 × 2 cm, *E*) afforded **1c** (294 mg, 78%). Colorless foam. TLC (*E*): R_f 0.9. ^{31}P-NMR ($CDCl_3$): 148.4, 148.5.

*1-[2-Deoxy-5-*O*-(4,4′-dimethoxytrityl)-β-*D*-*erythro*-pentofuranosyl]-3-(hex-1-ynyl)-1,5-dihydro-6-[(2-methylpropanoyl)amino]-4*H*-pyrazolo[3,4-*d*]pyrimidin-4-one 3′-(2-Cyanoethyl Diisopropylphosphoramidite)* (**1d**). As described for **1b**, with **6d** (150 mg, 0.21 mmol), THF (1 ml), (i-Pr)$_2$EtN (70 µl, 0.42 mmol), and 2-cyanoethyl diisopropylphosphoramidochloridite (62 µl, 0.27 mmol). FC (*E*) gave **1d** (152 mg, 79%). Colorless foam. TLC (*E*): R_f 0.9. ^{31}P-NMR ($CDCl_3$): 148.3, 149.4.

*3-Cyano-1-[2-deoxy-5-*O*-(4,4′-dimethoxytrityl)-β-*D*-erythro-pentofuranosyl]-1,5-dihydro-6-[(2-methylpropanoyl)amino]-4*H*-pyrazolo[3,4-*d*]pyrimidin-4-one 3′-(2-Cyanoethyl Diisopropylphosphoramidite)* (**2**). As described for **1b**, with **8** (100 mg, 0.15 mmol), THF (1 ml), $(i\text{-}Pr)_2EtN$ (75 µl, 0.45 mmol), and 2-cyanoethyl diisopropylphosphoramidochloridite (45 µl, 0.2 mmol). FC (*E*) gave **2** (92 mg, 72%). Colorless foam. TLC (*E*): R_f 0.9. ^{31}P-NMR ($CDCl_3$): 149.4, 149.7.

REFERENCES

[1] F. Seela, N. Ramzaeva, H. Rosemeyer, in 'Hetarenes', Houben-Weyl, Vol. E 9b, 'Bicyclic 6-Ring Systems Each with One to Two N-Atoms – Purines', Weinheim, 1997, p. 403.
[2] A. I. H. Murchie, D. M. J. Lilley, *EMBO J.* **1994**, *13*, 993.
[3] F. Seela, M. Zulauf, *Chem.–Eur. J.* **1998**, *4*, 1781.
[4] F. Seela, H. Driller, *Helv. Chim. Acta* **1988**, *71*, 1191.
[5] F. Seela, K. Kaiser, *Helv. Chim. Acta* **1988**, *71*, 1813.
[6] F. Seela, M. Zulauf, *J. Chem. Soc., Perkin Trans. 1* **1999**, 479.
[7] C. A. Buhr, R. W. Wagner, D. Grant, B. C. Froehler, *Nucleic Acids Res.* **1996**, *24*, 2974.
[8] G. Balow, V. Mohan, E. A. Lesnik, J. F. Johnston, B. P. Monia, O. L. Acevedo, *Nucleic Acids Res.* **1998**, *26*, 3350.
[9] D. Graham, J. A. Parkinson, T. Brown, *J. Chem. Soc., Perkin Trans. 1* **1998**, 1131.
[10] F. Seela, G. Becher, M. Zulauf, *Nucleosides Nucleotides* **1999**, *18*, 1399.
[11] F. Seela, G. Becher, *Chem. Commun*. **1998**, 2017.
[12] F. Seela, H. Steker, *Helv. Chim. Acta* **1986**, *69*, 1602.
[13] F. Seela, G. Becher, *Synthesis* **1998**, 207.
[14] N. Ramzaeva, G. Becher, F. Seela, *Synthesis* **1998**, 1327.
[15] R. F. Heck, *J. Am. Chem. Soc*. **1968**, *90*, 5518.
[16] F. Seela, G. Becher, H. Rosemeyer, H. Reuter, G. Kastner, I. A. Mikailopulo, *Helv. Chim. Acta* **1999**, *82*, 105.
[17] J. Plavec, 'Studies on the Stereoelectronic Effects in Nucleosides and Nucleotides', Thesis, Uppsala University, 1995.
[18] a) C. Hansch, A. Leo, R. W. Taft, *Chem. Rev* **1991**, *91*, 165; b) M. Oivanen, H. Lönnberg, X.-X. Zhon, J. Chattopadyaya, *Tetrahedron* **1987**, *43*, 1133.
[19] F. Jordan, H. Niv, *Nucleic Acids Res.* **1977**, *4*, 697.
[20] D. P. C. McGee, J. C. Martin, A. S. Webb, *Synthesis* **1983**, 540.
[21] J. Zemlicka, A. Holy, *Collect. Czech. Chem. Commun*. **1967**, *32*, 3159.
[22] H. Büchi, H. G. Khorana, *J. Mol. Biol*. **1972**, *72*, 251.
[23] H. Schaller, G. Weimann, B. Lerch, H. G. Khorana, *J. Am. Chem. Soc*. **1963**, *85*, 3821.
[24] A. D. Barone, J.-Y. Tang, M. H. Caruthers, *Nucleic Acids Res.* **1984**, *12*, 4051.
[25] N. D. Sinha, J. Biernat, J. McManus, H. Köster, *Nucleic Acids Res.* **1984**, *12*, 4539.
[26] F. Seela, M. Zulauf, *Nucleosides Nucleotides* **1999**, in press.
[27] B. C. Froehler, 'Protocols for Oligonucleotides and Analogs', in 'Methods in Molecular Biology', Ed. E. S. Agrawal, Humana Press, Totowa, N. J., 1994, Vol. 20, p. 63.
[28] Oligonucleotide Purification Cartridges, *Applied Biosystems*, Weiterstadt, Germany.
[29] Rainbow™ Universal CPG, *Clontech Laboratories Inc.*, Palo Alto, USA.
[30] L. Beigelman, *Ribozyme Pharmaceuticals Inc.*, Boulder, CO 80301, USA.
[31] C. R. Petrie, A. D. Adams, M. Stamm, J. Van Ness, S. M. Watanabe, R. B. Meyer, *Bioconjugate Chem*. **1991**, *2*, 441.
[32] F. Seela, H. Driller, *Nucleic Acids Res.* **1989**, *17*, 901.
[33] F. Seela, N. Ramzaeva, G. Becher, *Collect. Czech. Chem. Commun*. (Special Issue) **1996**, *61*, 258.
[34] F. Seela, M. Zulauf, *J. Chem. Soc., Perkin Trans. 2* **1998**, 3233.
[35] E. A. Lesnik, S. M. Freier, *Biochemistry* **1995**, *34*, 10807.
[36] N. Ramzaeva, C. Mittelbach, F. Seela, *Helv. Chim. Acta* **1997**, *80*, 1809.
[37] J. A. McDowell, D. H. Turner, *Biochemistry* **1996**, *35*, 14077.

Received June 17, 1999